A Biallelic Mutation in the Homologous Recombination Repair Gene SPIDR Is Associated With Human Gonadal Dysgenesis

Pola Smirin-Yosef,[1,2]* Nehama Zuckerman-Levin,[3,4]* Shay Tzur,[5,6] Yaron Granot,[5] Lior Cohen,[7,8,11] Juliane Sachsenweger,[9] Guntram Borck,[10] Irina Lagovsky,[2,11] Mali Salmon-Divon,[1] Lisa Wiesmüller,[9] and Lina Basel-Vanagaite[2,7,8,11]

[1]Genomic Bioinformatics Laboratory, Department of Molecular Biology, Ariel University, Ariel 40700, Israel; [2]Felsenstein Medical Research Center, Rabin Medical Center, Petah Tikva 4941492, Israel; [3]Clalit Health Services, Sharon-Shomron District 42505, Israel; [4]Pediatric Diabetes and Obesity Clinic, Rambam Medical Center, Bruce Rappaport Faculty of Medicine-Technion, Haifa 3200003, Israel; [5]Laboratory of Molecular Medicine, Rambam Health Care Campus, Haifa 3109601, Israel; [6]Genomic Research Department, Emedgene Technologies, Tel-Aviv 6789126, Israel; [7]Raphael Recanati Genetics Institute, Rabin Medical Center, Beilinson Campus, Petah Tikva 4941492, Israel; [8]Pediatric Genetics Unit, Schneider Children's Medical Center of Israel, Petah Tikva 49202, Israel; [9]Department of Obstetrics and Gynecology, Ulm University, Ulm 89075, Germany; [10]Institute of Human Genetics, ULM University, Ulm 89081, Germany; and [11]Sackler Faculty of Medicine, Tel Aviv University, Tel Aviv 6997801, Israel

Context: Primary ovarian insufficiency (POI) is caused by ovarian follicle depletion or follicle dysfunction, characterized by amenorrhea with elevated gonadotropin levels. The disorder presents as absence of normal progression of puberty.

Objective: To elucidate the cause of ovarian dysfunction in a family with POI.

Design: We performed whole-exome sequencing in 2 affected individuals. To evaluate whether DNA double-strand break (DSB) repair activities are altered in biallelic mutation carriers, we applied an enhanced green fluorescent protein-based assay for the detection of specific DSB repair pathways in blood-derived cells.

Setting: Diagnoses were made at the Pediatric Endocrine Clinic, Clalit Health Services, Sharon-Shomron District, Israel. Genetic counseling and sample collection were performed at the Pediatric Genetics Unit, Schneider Children's Medical Center Israel, Petah Tikva, Israel.

Patients and Intervention: Two sisters born to consanguineous parents of Israeli Muslim Arab ancestry presented with a lack of normal progression of puberty, high gonadotropin levels, and hypoplastic or absent ovaries on ultrasound. Blood samples for DNA extraction were obtained from all family members.

Main Outcome Measure: Exome analysis to elucidate the cause of POI in 2 affected sisters.

Results: Analysis revealed a stop-gain homozygous mutation in the *SPIDR* gene (*KIAA0146*) c.839G>A, p.W280*. This mutation altered SPIDR activity in homologous recombination, resulting in the accumulation of 53BP1-labeled DSBs postionizing radiation and γH2AX-labeled damage during unperturbed growth.

Conclusions: SPIDR is important for ovarian function in humans. A biallelic mutation in this gene may be associated with ovarian dysgenesis in cases of autosomal recessive inheritance. (***J Clin Endocrinol Metab*** **102: 681–688, 2017)**

ISSN Print 0021-972X ISSN Online 1945-7197
Printed in USA

Received 17 July 2016. Accepted 13 December 2016.
First Published Online 14 December 2016

*These authors contributed equally to this study.

Abbreviations: DSB, double-strand break; EGFP, enhanced green fluorescent protein; FACS, fluorescence-activated cell sorting; HR, homologous recombination; IR, ionizing radiation; NHEJ, nonhomologous end joining; PBL, peripheral blood lymphocyte; POI, primary ovarian insufficiency; SSA, single-strand annealing.

Primary ovarian insufficiency (POI) is a heterogeneous disorder caused by ovarian follicle dysfunction or depletion. POI results in the loss of ovarian function. Approximately 1% of women <40 years of age are affected by POI (1, 2), and in most cases, the etiology is unknown (3). The disorder presents as delayed puberty and is characterized by elevated gonadotropin levels (4, 5). The pathologic cascade might involve impaired ovarian formation, increased follicular atresia, impaired recruitment of dominant follicles, obstruction of follicular maturation, or rapid depletion of the follicular reserve (4, 5). Furthermore, POI may be an element of syndromes, such as Perrault syndrome, or it may occur in isolation (nonsyndromic POI).

Mutations in *GDF9*, *FIGLA*, *FSHR*, *NOBOX*, *NR5A1*, *NANOS3*, *STAG3*, *SYCE1*, *MCM8*, *MCM9*, and *HFM1* genes were found to cause POI with autosomal recessive or autosomal dominant inheritance modes (3). Some of these genes (*e.g.*, *MCM8*, *MCM9*) are involved in homologous recombination (HR) repair processes associated with POI (6).

HR is a metabolic process during the first meiotic division, required for accurate chromosome segregation. HR is found in all forms of life and constitutes a key repair and tolerance pathway for complex DNA damage, including DNA gaps, DNA interstrand cross-links, and DNA double-strand breaks (DSBs) (7).

In this study we found that a homozygous nonsense mutation in the *SPIDR* gene, encoding for a protein involved in homologous DNA repair, plays a role in an autosomal recessive POI in a consanguineous Israeli Muslim Arab family.

Materials and Methods

Clinical description of the subjects

Two daughters of consanguineous double first cousin parents of Arab ancestry were diagnosed with POI. The sisters, aged 12.6 years old (Fig. 1, p.1) and 14.8 years old (Fig. 1, p.2) were admitted to the Pediatric Endocrine Clinic, Clalit Health Services, Sharon-Shomron District, Israel, because of the absence of normal progression of puberty.

Their mother, a healthy 42-year-old woman, reported menarche at 12.5 years old. The mother's hormonal profile was normal, obstetric history was uneventful, and menstruation was regular. The 48-year-old father had a previous operation because of pheochromocytoma but was healthy at the time of the sisters' diagnosis. Both parents were of normal height (156 and 170 cm, respectively). The sisters had a healthy brother (Fig. 1, p.3) who presented normal clinical and hormonal progression of puberty. At 14.6 years of age, he had normal stature, was Tanner stage 5 of puberty, and had normal gonadotropin and testosterone levels. There was no family history of infertility, early menopause, or hearing loss.

The older daughter was admitted to the clinic at the age of 14.8 years old with lack of normal progression of puberty. A

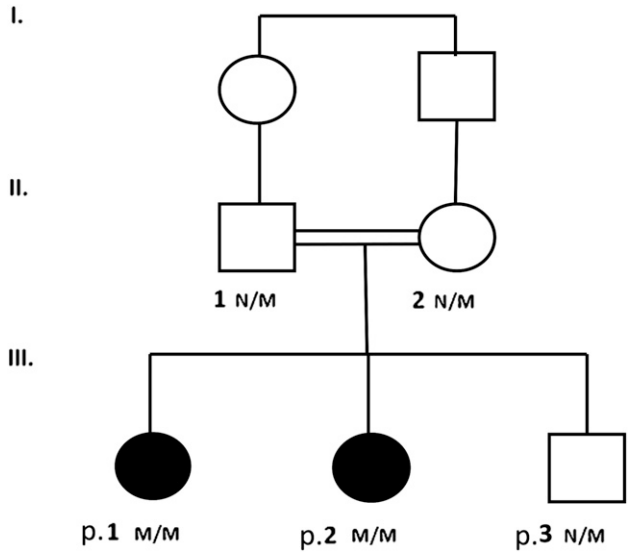

Figure 1. Pedigree of the family segregating for *SPIDR* p.W280* mutation. Individuals affected or likely to be affected are represented by filled black symbols. M, mutation; N, wild-type allele.

physical examination demonstrated normal height (156 cm, 22nd percentile for age), body mass index at 90th percentile for age (68 kg), and normal upper/lower segment ratio. Tanner staging for breast development and for pubic hair was 4 and 2, respectively. Breast development started at 12 years of age, and pubic hair appeared at the age of 11.5 years. The patient's hearing was normal, and she had no dysmorphic features. Serum gonadotropin concentrations were high on 2 consecutive measurements, with follicle stimulating hormone levels of 59.8 and 63 IU/L (normal, 1.0 to 14.7 IU/L), luteinizing hormone measurements of 30.3 and 29.4 IU/L (normal, 1.0 to 14.7 IU/L), and E2 of 138 pmol/L (normal, follicular 9 to 175 pmol/L). Testosterone and adrenal androgens, adrenocorticotropic hormone (ACTH) stimulation test, and steroid metabolomics by gas chromatography/mass spectrometry were normal.

A small prepubertal uterus ($1.9 \times 1.1 \times 4.3$ cm) was observed using a transabdominal ultrasound; ovaries could not be visualized. Bone age was that of a 13-year-old girl. On reevaluation of ovarian function, the level of estradiol was 85 pmol/L and that of the anti-Müllerian hormone was undetectable (<0.13 ng/mL). Chromosomal analysis revealed a normal karyotype (46,XX), and *FMR1* premutation testing was negative.

The younger daughter was admitted to the Pediatric Endocrine Clinic at 12.6 years of age because of her sister's history of gonadal insufficiency. After normal growth in early childhood, recent deceleration in growth was reported. At admission she was 142 cm tall (third percentile) and weighed 39 kg (26th percentile). Her physical examination revealed no abnormalities except for 2 abdominal café-au-lait spots. Tanner staging for breast development and pubic hair was 1. Hormonal testing showed high gonadotropin levels on 2 consecutive measurements: 102.2 and 85.8 IU/L for follicle stimulating hormone and 44.7 and 33.4 IU/L for luteinizing hormone. Serum E2 concentration was low (<70 pmol/L) and anti-Müllerian hormone was undetectable (<0.13 ng/mL). Testosterone, dehydroepiandrosterone, 17-OH progesterone, and androstenedione were normal. Additional testing included thyroid function tests, cortisol, and insulin-like growth factor 1 and insulin-like growth factor-binding protein levels, which were all normal. Bone age

was 11 to 11.5 years. A small prepubertal uterus measuring 1.19 × 1.34 × 3.95 cm and a left ovary measuring 0.81 × 1.04 cm were visualized by ultrasound. No follicles were detected, and the right ovary was not visualized. The results of chromosome analysis for this patient were normal for the female karyotype 46,XX and for the *FMR1* gene premutation test.

Increasing dosages (up to 1 mg) of estradiol hemihydrate were prescribed for both sisters and then replaced by estradiol hemihydrate/norethisterone acetate (Novofem® Bagsværd, Denmark), which induced regular menstruation.

At follow-up at the age of 19.6 years, the older sister, without medical recommendation, had stopped her hormonal replacement therapy for 7 months. Her hormonal profile remained abnormal, and no menstruation occurred during this time. No ovaries were demonstrated in an abdominal sonography.

Exome analysis

Informed consent was obtained from the patients and their parents according to the local Helsinki Committee and the National Committee for Genetic Studies, Israel Ministry of Health. DNA samples were isolated from family members' blood samples using standard protocols.

Analysis was performed at the Pediatric Genetics Unit, Schneider Children's Medical Center of Israel, Petah Tikva, Israel.

Library preparation was carried out using the TruSeq DNA Library Prep Kit (Illumina, San Diego, CA) followed by exome enrichment with the TruSeq Exome Enrichment Kit (FC-930-10 12; Illumina). Sequencing was performed on an Illumina HiSeq2000 platform in Gene by Gene Laboratories (Houston, TX). The emedgene bioinformatics platform (Tel Aviv, Israel) was used to analyze and interpret the next-generation sequencing (NGS) data. The platform filters out errors and polymorphic variants and identifies candidate variants, which are compatible with a family disease inheritance mode having the relevant phenotypic association. Sanger sequencing on an ABI 3100 Sequencer (Applied Biosystems, Foster City, CA) (using the primers F: 5′-TGGCCTCTGGGAAGATAATG-3′ and R: 5′-GCACAGATTGTGGTGATGTTTT-3′) was used to validate the variant and to perform cosegregation studies.

Blood samples and cell culture

Peripheral blood lymphocytes (PBLs) were isolated from heparinized blood samples by Ficoll 400 (Amersham Biosciences, Piscataway, NJ) gradient centrifugation. Washing in phosphate-buffered saline removed thrombocytes. Cells were then resuspended in PB-MAXTM Karyotyping Medium (Gibco/Invitrogen, Carlsbad, CA) containing 2% phytohemagglutinin (PAA, Pasching, Germany) and cultivated for 72 hours at 37°C.

DSB repair analyses

DSB repair was analyzed using our enhanced green fluorescent protein (EGFP)-based test system, as previously described (8, 9). In brief, DNA mixes containing a plasmid for the endonuclease I-SceI, 1 of the DSB repair substrates [Fig. 2(A)], and pBS filler plasmid (pBlueScriptII KS; Stratagene, Heidelberg, Germany) or wild-type EGFP expression plasmid (to determine transfection efficiency) were introduced by nucleofection according to the Amaxa protocol (Lonza, Cologne, Germany). Cells were then recultivated for 24 hours and harvested for fluorescence-activated cell sorting (FACS) analysis. Reconstitution of wild-type EGFP served as a measure of successful repair and was monitored via FACS analysis-based quantification of the fraction of green fluorescent cells. Live cells were gated in the side scatter/forward scatter dot plot, and green fluorescent cells were detected following laser excitation at 488 nm in the FL1/FL2 channels (FACS Calibur FACScan; BD, Heidelberg, Germany). Each quantification of green fluorescent cells in repair assays was normalized by using the individually determined transfection efficiency (20% to 30%) to calculate the DSB repair frequency.

Immunofluorescence microscopic analysis

PBLs were exposed to 2 Gy of ionizing radiation (IR) (Cs-137, GSR D1; Gamma-Service Medical GmbH, Leipzig, Germany) and harvested for the indicated time points posttreatment. They were then mounted on poly-L-lysine (Sigma-Aldrich, St. Louis, MO) slides and underwent cytospinning (Cytospin 3 Centrifuge; Shandon, Bohemia, NY) at 28 × g for 5 minutes. Cells were then fixed immediately with 3.7% formaldehyde, underwent permeabilization with 0.5% Triton X-100, were washed, and underwent blocking with 5% goat serum (Invitrogen, Karlsruhe, Germany) in phosphate-buffered saline. The primary antibodies were polyclonal anti-53BP1 (NB100-304; Novus Biologicals, Littleton, CO) and anti-γH2AX (Ser139, clone JBW301; Millipore, Billerica, MA); secondary antibody was AlexaFluor555 labeled (Invitrogen). Nuclear counterstaining was performed with 4′,6-diamidino-2-phenylindole; coverslips were mounted with VectaShield mounting media (Vector Laboratories, Burlingame, CA). Immunofluorescence was visualized with a BZ-9000 microscope (Keyence, Neu-Isenburg, Germany) and analyzed by BZ-II Analyzer software (Keyence).

Cellular sensitivity to poly ADP ribose polymerase inhibition and carboplatin

PBLs were treated 3 times over 7 days with various poly ADP ribose polymerase inhibitor 1,5-isoquinolinediol (IQD, Enzo Life Sciences, New York, NY) concentrations ranging from 1 μM to 2 mM. Sensitivity to carboplatin was examined after exposure to 0.125 μM to 2 mM carboplatin for 24 hours, followed by cultivation for 24 hours in fresh medium. Cell viability posttreatment was determined in duplicates using the 3-(4,5-dimethylthiazol-2-yl)-2,5-diphenyltetrazolium bromide assay previously described (10). Statistical significance was determined with the F test using Graphpad Prism 5.01 (GraphPad, San Diego, CA).

Results

The list of candidate genes focused on functional variants (*e.g.*, missense, nonsense, frameshift, splicing), with a minor allele frequency <1% in Europeans (based on the 1000 Genomes Project and ESP6500) and which are presumably deleterious. According to the hypothesis of a homozygous recessive mode of inheritance, we identified 9 homozygous variants in both affected individuals (Supplemental Table 2). We prioritized these genes based on their known functions and on the statistical properties of the genes (*e.g.*, number of loss of function, conservations, residual variation intolerance score). Two variants were ruled out because of high residual variation

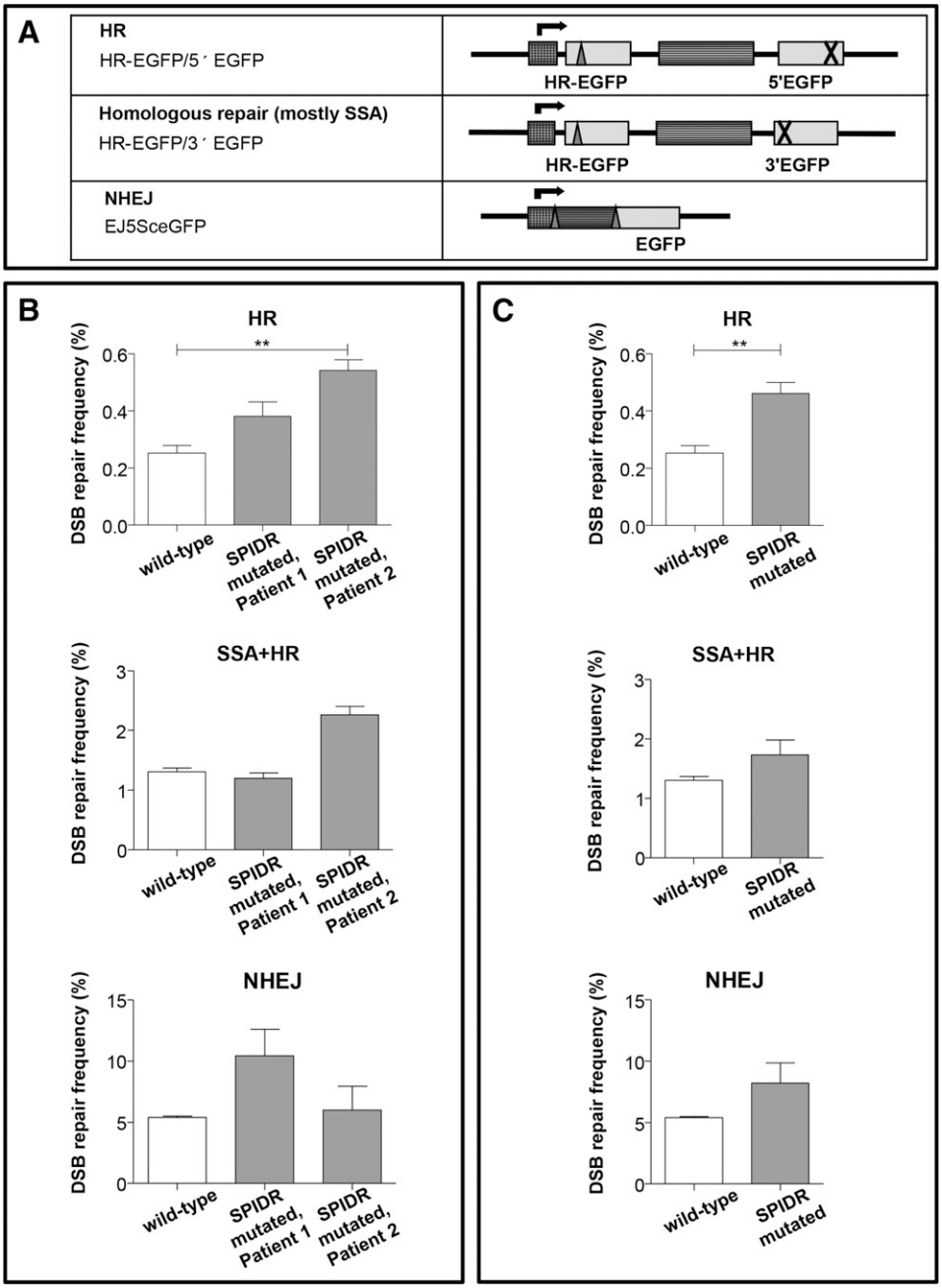

Figure 2. Analysis of DSB repair and recombination activities in individuals with wild-type and homozygous mutated *SPIDR*. (A) Schematic presentation of DSB repair substrates (8). To measure HR, we used substrate HR-EGFP/5′EGFP, consisting of a mutated acceptor *EGFP* gene, which lacks 4 bp of the EGFP gene at the position, where the I-*Sce*I restriction sequence was inserted and a 3′ truncated 5′EGFP, which serves as a donor sequence. DSB repair substrate HR-EGFP/3′EGFP was designed to measure homologous repair (*i.e.*, mostly SSA under the assay conditions). The donor 3′EGFP gene variant was mutated at the start codon. For NHEJ evaluation, we used plasmid EJ5SceGFP with 2 tandem I-*Sce*I cutting sequences encompassing a spacer sequence separating the transcriptional promoter from the *EGFP* coding sequence. I-*Sce*I, is indicated by the triangle; cross, inactivating mutation/truncation; light gray bars, EGFP variant genes; gray stripes bars, spacer sequences; and gray dots bar with kinked arrow, transcriptional promoter. (B and C) DSB repair measurements. Percentages of EGFP-positive live cells were normalized to the individually determined transfection efficiencies for DSB repair frequency calculations. Mean values and standard error of the mean from 3 to 6 measurements are shown. Statistically significant differences were determined using the nonparametric Mann-Whitney *U* test for unpaired samples with GraphPad Prism 5.01 software. $^{**}P < 0.01$. (B) Comparison between DSB repair in each individual. (C) Comparison of DSB repair frequencies from Fig. 2(B) summarized as a function of the *SPIDR* gene status.

intolerance. Two were ruled out because the amino acid sequence was not conserved. Four were ruled out for irrelevance to the patient phenotype. This filtering procedure ended with a single homozygous nonsense mutation in the *SPIDR* (*KIAA0146*) gene, which encodes for a scaffolding protein involved in DNA repair and has a function in HR. The mutation p.W280* (NM_001080394.2:c.839G>A) is a stop-gain variant

in the transcript NM_001080394.2, located in chromosome 8q (in chr8:g.48,320,485G>A, hg19) within a homozygotic chromosomal segment of 18mbp (chr8: g.39,370,135-57,353,826, hg19). This variant in a homozygous state was not observed in any of the controls of Muslim Arab individuals in our local database (n = 252). Moreover, this variant has never been reported in public cohorts, including the ExAC database (11). The mutation was validated in all family members, with familial segregation compatible with an autosomal recessive mode of inheritance: the affected daughters were homozygotes, and the parents and the healthy brother were heterozygotes (Fig. 1).

The stop-gain mutation found in *SPIDR* might lead to either nonsense-mediated decay of the mutated messenger RNA (NMD) or to the production of a truncated protein, in the middle of a domain that is necessary for interaction with RAD51 (UniProtKB: Q14159). The *SPIDR* coding region contains 2214 nucleotides (738 codons); the translated product of the mutated gene is predicted to be a shorter protein containing only 38% of the native one. Out of the 60,000 individuals comprising the ExAC database (11), not one had a homozygous predicted loss of function variant in the *SPIDR* gene. Considering the predicted impact of the *SPIDR* mutation and its gene function described herein, the other candidates found in the analysis were discarded as not likely to be responsible for the disease (12) (Supplemental Table 2). In addition, we found 72 functional rare heterozygous variants in 64 genes (annotation was performed using ANNOVAR; http://annovar.openbioinformatics.org/en/latest/); none was associated with POI (data not shown).

To evaluate whether DNA DSB repair activities are altered in mutation carriers, we applied an EGFP-based assay for the detection of specific DSB repair pathways in blood-derived cells (9, 13–15). Given that *SPIDR* has been linked with HR (16), we first addressed this DSB repair pathway in fresh PBLs. In parallel, we tested single-strand annealing (SSA) and nonhomologous end joining (NHEJ)—2 DSB repair pathways known to compensate for loss of HR function—in cells derived from *BRCA1*, *BRCA2*, and *PALB2* mutation carriers (9, 13, 14) [Fig. 2(A)]. HR analysis revealed a 1.5-fold enhanced HR (P = 0.0931) in p.1 and a 2.1-fold statistically significant HR increase in p.2 (P = 0.0022) compared with the healthy sibling [Fig. 2(B)]. Using a reporter construct that under the transient assay conditions mostly detects SSA (13) or an NHEJ construct, a significant change was not observed ($P \geq 0.1000$). Comparison of mean values for mutated (average from p.1 and p.2) vs wild-type (healthy sibling) status confirmed the HR increase in *SPIDR* mutation carriers (P = 0.0076) [Fig. 2(C)]. Percentages of living cells (side scatter/forward scatter gate in FACS dot plot) were comparable in the samples from the mutation carriers and the unaffected sibling, excluding a potential bias by differences in survival (data not shown). Moreover, each value for EGFP positivity in live cells was corrected for the individually determined transfection efficiency, further excluding indirect effects from transfection, growth, or expression.

To better understand potential effects of the *SPIDR* mutation on the DNA damage response in the chromatin context, we monitored the kinetics of focal accumulations (foci) of the DNA binding protein 53BP1 and the DNA damage marker γH2AX. One hour after IR treatment, 53BP1 foci were accumulated in PBLs from the 3 cell types, suggesting a comparable DSB formation (Fig. 3). Six hours post-IR, that is after the early DSB repair phase mostly characterized by canonical NHEJ (17), 53BP1 foci further accumulated in *SPIDR*-mutated PBLs, resulting in a statistically significant 53BP1 foci increase in both patients as compared with the unaffected sibling (an average increase of 1.5-fold, $P < 0.0001$). Interestingly, no consistent foci increase was observed when analyzing γH2AX foci at the critical time point, 6 hours post-IR. However, in both *SPIDR* mutation carrier samples, basal DNA damage levels, as indicated by γH2AX foci in untreated cells, were significantly elevated by an average of 2.8-fold ($P < 0.0001$). Taken together, these data suggest that the newly identified mutation altered SPIDR activities in HR, resulting in the accumulation of 53BP1-labeled DSBs post-IR and of γH2AX-labeled damage during unperturbed growth.

Discussion

Chromosomal abnormalities occurring during meiosis are a common cause of POI. DNA repair of these abnormities by HR is an essential process for normal ovarian development; mutations in genes involved in HR repair may lead to POI (3). SPIDR is involved in HR repair and is most highly expressed in the ovary (18). SPIDR-depleted cells have higher rates of sister chromatid exchange, defects in HR, and higher levels of genome instability (16). Mutations of other genes involved in HR repair and chromosomal instability during meiosis have been found previously to cause POI in humans. These include *HFM1* (19), *MCM8* (20), *MCM9* (21), *SYCE1* (22), and *STAG3*, which are essential for pairing and segregation of chromosomes (23).

The clinical phenotype of POI varies, even within a single family with the same mutation (22, 24–26): it can present as delayed puberty, lack of normal progression of puberty, primary or secondary amenorrhea, and/or premature menopause. The patients in this study had the same mutation but differed in their clinical presentation.

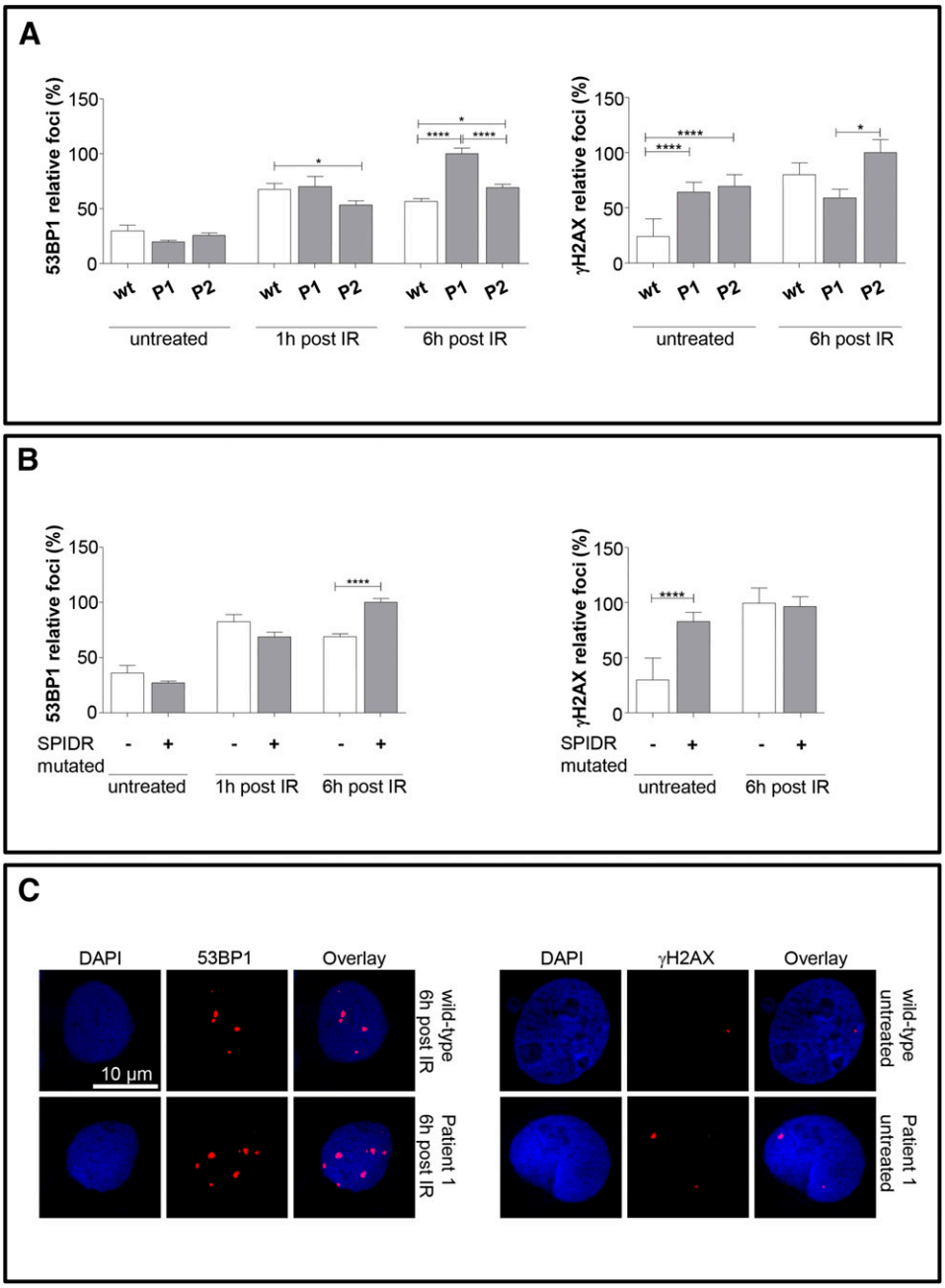

Figure 3. Analysis of DNA damage signals based on immunofluorescence microscopy. Focal accumulation of the DNA damage marker 53BP1 and γH2AX in the nuclei was analyzed at the indicated time points post-IR (2 Gy) or in untreated samples. Immunolabeled foci from 50 to 400 nuclei were scored by automated quantification for each slide. $*P < 0.05$; $****P < 0.0001$. (A) Comparison of 53BP1 and γH2AX foci formation between individuals. Maximum mean scores were defined as 100% (absolute mean values for 53BP1, 7 foci per cell; absolute mean values for γH2AX, 2 foci per cell). P1, patient 1 with homozygous *SPIDR* mutation; P2, patient 2 with homozygous *SPIDR* mutation; wt, wild type. (B) Comparison of 53BP1 and γH2AX foci formation from Figure 3(A), summarized as a function of the *SPIDR* gene status. (C) Representative images for 53BP1 and γH2AX foci quantification 6 h post-IR and in untreated samples, respectively.

Genes that are involved in meiotic recombination disruption that results in female sterility have also been found in mice [*e.g.*, *Msh4* or *Msh5* (27), *Dmc1*, *Spo11* (28)].

SPIDR protein directly interacts with proteins that are involved in gonadal disorders, including FIGNL1 protein, which acts in the HR repair process (29); when impaired, FIGNL1 reduces testis weight in mice (30). SPIDR also directly interacts with the BLM protein (16), which when mutated leads to Bloom syndrome, reducing female fertility (31) and decreasing the reproductive period. SPIDR, which promotes the formation of a BLM-/RAD51-containing complex (16), is of particular interest because the POI genes *MCM8* and *MCM9* (20, 21) are related to RAD51 recruitment at DNA damage sites to facilitate HR (32).

In PBLs from *SPIDR* mutation carriers, we observed aberrantly enhanced HR, which is compatible with

elevated sister chromatid exchanges, normally suppressed by the SPIDR complex partner BLM (16). Expression of a truncated SPIDR protein may differ from complete loss of SPIDR, which was reported to result in an HR decrease (16). SPIDR was proposed to coordinate HR via *N*-terminal RAD51 binding, promoting RAD51 loading on resected DNA and via C-terminal BLM interactions, promoting resolution of crossover intermediates (16, 29). The *SPIDR* mutation completely deleted the C-terminal BLM binding site and is compatible with a more prominent loss of BLM-mediated HR repression as compared with RAD51-dependent HR promoting functions. On the other hand, partial loss of the *N*-terminal RAD51 binding site may explain why 53BP1, but not γH2AX foci, accumulated in PBLs from mutation carriers post-IR. Although γH2AX foci are indiscriminately generated at DSBs, 53BP1 is known to form part of a DNA end-binding complex, antagonizing HR particularly in cases of an endogenous defect, thus indicating HR dysfunction in the *SPIDR*-mutated cells (33). γH2AX was reported to reflect different types of DNA damage, including DNA replication blocking lesions, which can be resolved by HR mechanisms (34). A rise of γH2AX, but not 53BP1 foci, during unperturbed growth of patient cells therefore likely reflects unresolved replication lesions. Our data suggest reduced HR functions, particularly at replication forks, and concomitantly compromised HR control mechanisms exerted by BLM.

Overall, the POI phenotype of *SPIDR* is supported by loss of function by this type of mutation (stop-gain), family segregation, expression in ovary, and most importantly, its involvement in HR repair.

In summary, 2 sisters affected with POI from a consanguineous Muslim Arab family were found to carry a homozygous nonsense mutation in the *SPIDR* gene, which is involved in homologous DNA repair. Based on these results, we conclude that SPIDR is important for ovarian function in humans and that biallelic mutation of SPIDR is associated with an autosomal recessive ovarian dysgenesis.

Acknowledgments

The authors are grateful for the support of The Milken Family Foundation and The Lowell Milken Family Foundation for providing the scholarship for P.-S.Y.

Address all correspondence and requests for reprints to: Lina Basel-Vanagaite, MD, PhD, Pediatric Genetics Unit, Schneider Children's Medical Center of Israel, Petah Tikva 49202, Israel. E-mail: basel@post.tau.ac.il.

Disclosure Summary: S.T. is the CSO and cofounder of Emedgene Technologies Ltd. The remaining authors have nothing to disclose.

References

1. Coulam CB, Adamson SC, Annegers JF. Incidence of premature ovarian failure. *Obstet Gynecol*. 1986;**67**(4):604–606.
2. Rebar RW, Connolly HV. Clinical features of young women with hypergonadotropic amenorrhea. *Fertil Steril*. 1990;**53**(5):804–810.
3. Qin Y, Jiao X, Simpson JL, Chen Z-J. Genetics of primary ovarian insufficiency: new developments and opportunities. *Hum Reprod Update*. 2015;**21**(6):787–808.
4. Nelson LM. Clinical practice. Primary ovarian insufficiency. *N Engl J Med*. 2009;**360**(6):606–614.
5. De Vos M, Devroey P, Fauser BCJM. Primary ovarian insufficiency. *Lancet*. 2010;**376**(9744):911–921.
6. Lutzmann M, Grey C, Traver S, Ganier O, Maya-Mendoza A, Ranisavljevic N, Bernex F, Nishiyama A, Montel N, Gavois E, Forichon L, de Massy B, Méchali M. MCM8- and MCM9-deficient mice reveal gametogenesis defects and genome instability due to impaired homologous recombination. *Mol Cell*. 2012;**47**(4):523–534.
7. Heyer W-D, Ehmsen KT, Liu J. Regulation of homologous recombination in eukaryotes. *Annu Rev Genet*. 2010;**44**:113–139.
8. Akyüz N, Boehden GS, Süsse S, Rimek A, Preuss U, Scheidtmann K-H, Wiesmüller L. DNA substrate dependence of p53-mediated regulation of double-strand break repair. *Mol Cell Biol*. 2002;**22**(17):6306–6317.
9. Obermeier K, Sachsenweger J, Friedl TWP, Pospiech H, Winqvist R, Wiesmüller L. Heterozygous PALB2 c.1592delT mutation channels DNA double-strand break repair into error-prone pathways in breast cancer patients. *Oncogene*. 2016;**35**(29):3796–3806.
10. Ireno IC, Wiehe RS, Stahl AI, Hampp S, Aydin S, Troester MA, Selivanova G, Wiesmüller L. Modulation of the poly (ADP-ribose) polymerase inhibitor response and DNA recombination in breast cancer cells by drugs affecting endogenous wild-type p53. *Carcinogenesis*. 2014;**35**(10):2273–2282.
11. Consortium EA, Lek M, Karczewski K, Minikel E, Samocha K, Banks E, Fennell T, O'Donnell-Luria A, Ware J, Hill A, Cummings B, Tukiainen T, Birnbaum D, Kosmicki J, Duncan L, Estrada K, Zhao F, Zou J, Pierce-Hoffman E, Berghout J, Cooper D, Deflaux N, DePristo M, Do R, Flannick J, Fromer M, Gauthier L, Goldstein J, Gupta N, Howrigan D, Kiezun A, Kurki M, Moonshine AL, Natarajan P, Orozco L, Peloso G, Poplin R, Rivas M, Ruano-Rubio V, Rose S, Ruderfer D, Shakir K, Stenson P, Stevens C, Thomas B, Tiao G, Tusie-Luna M, Weisburd B, Won H-H, Yu D, Altshuler D, Ardissino D, Boehnke M, Danesh J, Donnelly S, Roberto E, Florez J, Gabriel S, Getz G, Glatt S, Hultman C, Kathiresan S, Laakso M, McCarroll S, McCarthy M, McGovern D, McPherson R, Neale B, Palotie A, Purcell S, Saleheen D, Scharf J, Sklar P, Sullivan P, Tuomilehto J, Tsuang M, Watkins H, Wilson J, Daly M, MacArthur D. Analysis of protein-coding genetic variation in 60,706 humans. *Cold Spring Harbor Labs Journals*. 2015;**536**:285–291.
12. Petrovski S, Wang Q, Heinzen EL, Allen AS, Goldstein DB. Genic intolerance to functional variation and the interpretation of personal genomes. *PLoS Genet*. 2013;**9**(8):e1003709.
13. Keimling M, Deniz M, Varga D, Stahl A, Schrezenmeier H, Kreienberg R, Hoffmann I, König J, Wiesmüller L. The power of DNA double-strand break (DSB) repair testing to predict breast cancer susceptibility. *FASEB J*. 2012;**26**(5):2094–2104.
14. Keimling M, Volcic M, Csernok A, Wieland B, Dörk T, Wiesmüller L. Functional characterization connects individual patient mutations in ataxia telangiectasia mutated (ATM) with dysfunction of specific DNA double-strand break-repair signaling pathways. *FASEB J*. 2011;**25**(11):3849–3860.
15. Gatz SA, Salles D, Jacobsen E-M, Dörk T, Rausch T, Aydin S, Surowy H, Volcic M, Vogel W, Debatin K-M, Stütz AM, Schwarz K, Pannicke U, Hess T, Korbel JO, Schulz AS, Schumacher J, Wiesmüller L. MCM3AP and POMP mutations cause a DNA-repair and DNA-damage-signaling defect in an immunodeficient child. *Hum Mutat*. 2016;**37**(3):257–268.

16. Wan L, Han J, Liu T, Dong S, Xie F, Chen H, Huang J. Scaffolding protein SPIDR/KIAA0146 connects the Bloom syndrome helicase with homologous recombination repair. *Proc Natl Acad Sci USA*. 2013;**110**(26):10646–10651.
17. Riballo E, Kühne M, Rief N, Doherty A, Smith GCM, Recio M-J, Reis C, Dahm K, Fricke A, Krempler A, Parker AR, Jackson SP, Gennery A, Jeggo PA, Löbrich M. A pathway of double-strand break rejoining dependent upon ATM, Artemis, and proteins locating to gamma-H2AX foci. *Mol Cell*. 2004;**16**(5):715–724.
18. Wu C, Orozco C, Boyer J, Leglise M, Goodale J, Batalov S, Hodge CL, Haase J, Janes J, Huss JW III, Su AI. BioGPS: an extensible and customizable portal for querying and organizing gene annotation resources. *Genome Biol*. 2009;**10**(11):R130.
19. Wang J, Zhang W, Jiang H, Wu B-L; Primary Ovarian Insufficiency Collaboration. Mutations in HFM1 in recessive primary ovarian insufficiency. *N Engl J Med*. 2014;**370**(10):972–974.
20. AlAsiri S, Basit S, Wood-Trageser MA, Yatsenko SA, Jeffries EP, Surti U, Ketterer DM, Afzal S, Ramzan K, Faiyaz-Ul Haque M, Jiang H, Trakselis MA, Rajkovic A. Exome sequencing reveals MCM8 mutation underlies ovarian failure and chromosomal instability. *J Clin Invest*. 2015;**125**(1):258–262.
21. Wood-Trageser MA, Gurbuz F, Yatsenko SA, Jeffries EP, Kotan LD, Surti U, Ketterer DM, Matic J, Chipkin J, Jiang H, Trakselis MA, Topaloglu AK, Rajkovic A. MCM9 mutations are associated with ovarian failure, short stature, and chromosomal instability. *Am J Hum Genet*. 2014;**95**(6):754–762.
22. de Vries L, Behar DM, Smirin-Yosef P, Lagovsky I, Tzur S, Basel-Vanagaite L. Exome sequencing reveals SYCE1 mutation associated with autosomal recessive primary ovarian insufficiency. *J Clin Endocrinol Metab*. 2014;**99**(10):E2129–E2132.
23. Caburet S, Arboleda VA, Llano E, Overbeek PA, Barbero JL, Oka K, Harrison W, Vaiman D, Ben-Neriah Z, García-Tuñón I, Fellous M, Pendás AM, Veitia RA, Vilain E. Mutant cohesin in premature ovarian failure. *N Engl J Med*. 2014;**370**(10):943–949.
24. Zangen D, Kaufman Y, Zeligson S, Perlberg S, Fridman H, Kanaan M, Abdulhadi-Atwan M, Abu Libdeh A, Gussow A, Kisslov I, Carmel L, Renbaum P, Levy-Lahad E. XX ovarian dysgenesis is caused by a PSMC3IP/HOP2 mutation that abolishes coactivation of estrogen-driven transcription. *Am J Hum Genet*. 2011;**89**(4):572–579.
25. Tenenbaum-Rakover Y, Weinberg-Shukron A, Renbaum P, Lobel O, Eideh H, Gulsuner S, Dahary D, Abu-Rayyan A, Kanaan M, Levy-Lahad E, Bercovich D, Zangen D. Minichromosome maintenance complex component 8 (MCM8) gene mutations result in primary gonadal failure. *J Med Genet*. 2015;**52**(6):391–399.
26. Beysen D, De Paepe A, De Baere E. FOXL2 mutations and genomic rearrangements in BPES. *Hum Mutat*. 2009;**30**(2):158–169.
27. de Vries SS, Baart EB, Dekker M, Siezen A, de Rooij DG, de Boer P, te Riele H. Mouse MutS-like protein Msh5 is required for proper chromosome synapsis in male and female meiosis. *Genes Dev*. 1999;**13**(5):523–531.
28. Mandon-Pépin B, Touraine P, Kuttenn F, Derbois C, Rouxel A, Matsuda F, Nicolas A, Cotinot C, Fellous M. Genetic investigation of four meiotic genes in women with premature ovarian failure. *Eur J Endocrinol*. 2008;**158**(1):107–115.
29. Yuan J, Chen J. FIGNL1-containing protein complex is required for efficient homologous recombination repair. *Proc Natl Acad Sci USA*. 2013;**110**(26):10640–10645.
30. L'Hôte D, Vatin M, Auer J, Castille J, Passet B, Montagutelli X, Serres C, Vaiman D. Fidgetin-like1 is a strong candidate for a dynamic impairment of male meiosis leading to reduced testis weight in mice. *PLoS One*. 2011;**6**(11):e27582.
31. German J. Bloom syndrome: a mendelian prototype of somatic mutational disease. *Medicine (Baltimore)*. 1993;**72**(6):393–406.
32. Park J, Long DT, Lee KY, Abbas T, Shibata E, Negishi M, Luo Y, Schimenti JC, Gambus A, Walter JC, Dutta A. The MCM8-MCM9 complex promotes RAD51 recruitment at DNA damage sites to facilitate homologous recombination. *Mol Cell Biol*. 2013;**33**(8):1632–1644.
33. Panier S, Boulton SJ. Double-strand break repair: 53BP1 comes into focus. *Nat Rev Mol Cell Biol*. 2014;**15**(1):7–18.
34. Sedelnikova OA, Redon CE, Dickey JS, Nakamura AJ, Georgakilas AG, Bonner WM. Role of oxidatively induced DNA lesions in human pathogenesis. *Mutat Res*. 2010;**704**(1-3):152–159.